FAST AND EFFICIENT REJECTION OF BACKGROUND WAVEFORMS IN INTERICTAL EEG

Elham Bagheri[a], Jing Jin[a], Justin Dauwels[a], Sydney Cash[b], M.Brandon Westover[b]

[a] Nanyang Technological University, School of Electrical and Electronic Engineering, Singapore 639798

[b] Neurology Department, Massachusetts General Hospital, Boston, MA, USA, and Harvard Medical School, Cambridge, MA, USA

ABSTRACT

Automated annotation of electroencephalograms (EEG) of epileptic patients is important in diagnosis and management of epilepsy. Epilepsy is often associated with the presence of epileptiform transients (ET) in the EEG. To develop an efficient ET detector, a vast amount of data is required to train and evaluate the performance of the detector. Interictal EEG data contains mostly background waveforms, since ETs only occur occasionally in most patients. In order to detect ETs in an automated fashion, it is meaningful to first try to eliminate most background waveforms by means of simple, fast classifiers. The remaining waveforms can in a following step be processed by more sophisticated and computationally demanding classification algorithms, such as deep learning systems. In this study, we design a cascade of simple thresholding steps to reject most background waveforms in interictal EEG, while maintaining most ETs. Several simple and quick-to-compute EEG features are chosen. By thresholding these features in consecutive steps, background waveforms are rejected sequentially. In our numerical experiments, a cascade of 10 steps is able to reject 98.65% of all background segments in the dataset, while preserving 90.6% of the ETs.

Index Terms— Spike Detection; Electroencephalogram; Interictal Discharges; Epileptiform Transients; Epilepsy

1. INTRODUCTION

Electroencephalograms (EEGs) of patients with epilepsy might be characterized by epileptiform transients (ETs), also called interictal discharges, occurring between seizures [1, 2]. ETs are spikes or sharp waves with pointed peaks, which can last for 20-70 ms and 70-200 ms, respectively. The presence of ETs in EEG is often associated with epilepsy, therefore, ETs are instrumental in the diagnosis of epilepsy. Traditionally, experts detect the ETs from EEG recordings by visual inspection, which is very time consuming. Moreover, there is substantial disagreement between experts in EEG interpretation. Consequently, automated ET detection is sorely needed, and will increase the uniformity in EEG interpretation of epileptic patients [2].

Several methods have been applied for automated ET detection, including template matching, parametric methods, mimetic analysis, power spectral analysis, wavelet analysis, and artificial neural networks [2]. In addition, several other methods have been reported more recently [3, 4, 5, 6]. These methods use template matching in combination with clustering [3], template matching in combination with support vector machines (SVMs) [4], nonlinear energy operator in conjunction with mimetic analysis and Adaboost classifiers [5], and sequence merging followed by SVMs [6]. However, the common problem with these methods is the lack of a sizable database of different ET profiles to validate the performance of the ET detection systems. Therefore, the results are not reliable for clinical purposes.

In this study, a database of routine EEG recordings from 100 epileptic patients is analyzed. In order to be able to cope with this vast volume of data, we develop a system of simple classifiers to eliminate most of the background waveforms in the EEGs. After this processing step the remaining EEG waveforms can be analyzed by more complex and powerful machine learning procedures. However, the latter falls beyond the scope of this paper. Here we describe how we designed a cascade of simple classifiers for fast rejection of background waveforms. Since ET characteristics are of great variety, the proposed method consists of multiple stages to reject the background waveforms, and each stage makes use of one specific feature. The general idea behind the proposed method is illustrated in Fig. 1. Our numerical results show that this cascade of thresholding steps is able to reject 98.65% of the background waveforms in (interictal) EEG of epilepsy patients, while preserving 90.6% of the ETs.

This paper is organized as follows. In Section 2 we describe the EEG dataset, review relevant EEG features, and explain how we designed the cascade of thresholding steps. In Section 3 we present our results, and in Section 4 we offer concluding remarks.

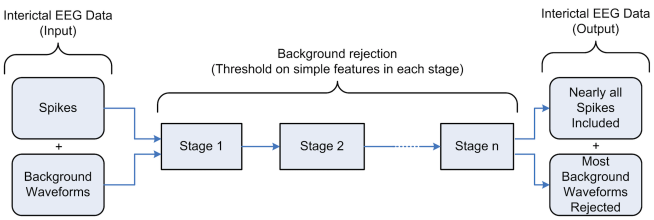

Fig. 1: Schematic of background rejection method.

2. MATERIALS AND METHODS

2.1. Scalp EEG data

In this study, we consider 30min EEG recordings of 100 patients with epilepsy. The data was acquired at the Massachusetts General Hospital (MGH), using the international 10-20 system of electrode placement. The sampling frequency is 128Hz and a notch filter at 60HZ is applied to remove the power line interference. In addition, it has been high-pass filtered by cut-off frequency of 0.1 Hz to remove the baseline. Data is cross-annotated using EEG annotation software SpikeGUI [7] by two neurologists from MGH. There is a total number of 19,255 ETs in the dataset.

2.2. Feature extraction

The EEG recordings are divided into segments of 0.5s, corresponding to 64 samples. The feature values are computed for each of these segments. Only waveforms that are labeled as ETs by both annotators are considered as ETs. Only the waveforms that do not have overlap with ETs are considered as background waveforms.Waveforms that overlap with ETs, in the same channel or any of the neighboring channels, are not considered as background waveforms. It is noteworthy that there might be ETs with lower peaks in channels near to annotated ETs. These low-amplitude ETs might be missed by the annotators. Our approach of selecting background waveforms ensures that these low-amplitude ETs are not treated as background waveforms. This is particularly important in the training phase, where we need to determine a suitable threshold for discriminating between ETs and background waveforms.

2.2.1. Morphological features

Morphological features include peak voltage, rising and falling voltages and slopes, and line length. The line length of an N-point signal $x(n)$ is computed as [8]:

$$L = \Sigma_{i=1}^{N} |(x(k-1) - x(k))|. \tag{1}$$

To compute the voltage and slope values, we first search for the ET peak in each segment of the data. Next we compute the neighboring troughs, and calculate the required voltages and slopes accordingly. Fig. 2 illustrates the computation of morphological features.

2.2.2. Nonlinear energy operator

The nonlinear energy operator (NLEO) has been shown to be effective in ET detection [9]. NLEO for discrete time signal $x(n)$ is defined as:

$$\psi_k\{x(n)\} = x^2(n) - x(n-k)x(n+k), \tag{2}$$

where k is the resolution parameter [10]. We choose k ranging from 1 to 32. To extract this feature, the NLEO value is first computed for each sample point in the EEG time series data.The NLEO for each 0.5s segment is defined as the maximum absolute NLEO value within that segment.

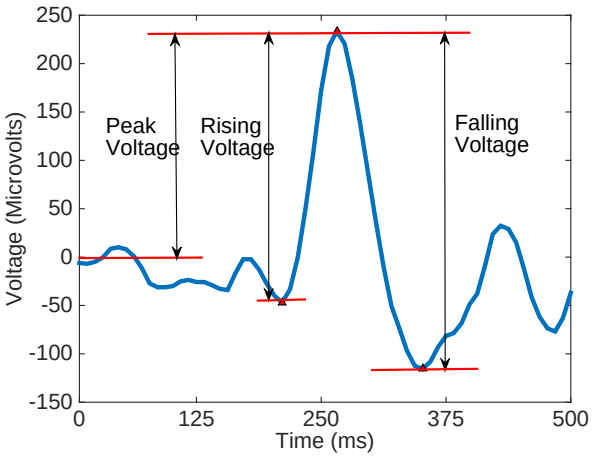

Fig. 2: Morphological features of an ET.

2.2.3. Wavelet transform

We apply both the continuous wavelet transform (CWT) and the discrete wavelet transform (DWT). Multiple mother wavelets including Symlets, Coiflets, and Daubechies families with different degrees were tested. We chose the mother wavelet that led to the highest background rejection rate; this turned out to be the Daubechies 3 (DB3) mother wavelet. In the CWT, the signal is compared with the shifted, compressed and stretched forms of a mother wavelet. The CWT of a signal $f(t)$ using mother wavelet $\psi(t)$ is given as:

$$C(u,s) = \frac{1}{\sqrt{s}} \int_{-\infty}^{\infty} f(t)\psi(\frac{t-u}{s})dt, \tag{3}$$

where s and u represent the scaling and translation parameters, respectively. The wavelet coefficient C for $\psi_{u,s}(x)$ defines shifting and scaling of the mother wavelet:

$$\psi_{u,s}(t) = \frac{1}{\sqrt{s}}\psi(\frac{t-u}{s}). \tag{4}$$

Compression or stretching is determined by the scale factor s [11]. We apply different values of the scale factor s, ranging from 1 to 30.

In the discrete wavelet transform (DWT), the signal is decomposed into multiple scales. Fig. 3 shows the multiscale decomposition of the signal $x[n]$ obtained by DWT, where $g(n)$ and $f(n)$ are high-pass and low-pass filters, respectively. The parameter D_i is the detail, whereas A_i represents the approximation at the ith level [12].

In this study, the DWT is applied over 4 levels, and the detail and approximation coefficients are calculated for all levels. We first compute the DTW for the entire EEG recordings. Next we extract the DTW coefficient for each 0.5s segment. In this way, we can avoid potential distortions at the boundaries of the segments. The maximum absolute value of the coefficients within each segment is defined as the feature.

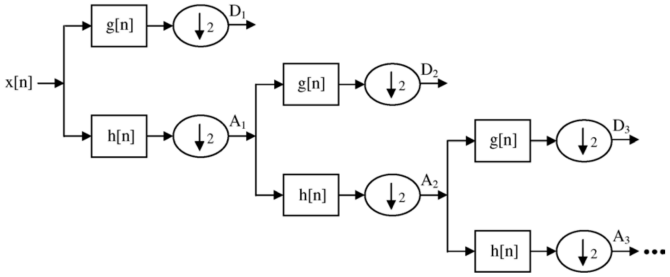

Fig. 3: Subband decomposition of discrete wavelet transform implementation [12].

2.2.4. Features in different frequency bands

Besides extracting features for bandpass-filtered signals between 0.1 to 64 Hz, all the aforementioned features are computed in 5 standard EEG bands: Delta (<4 Hz), Theta (4–8 Hz), Alpha (8–12 Hz), Beta (12–32 Hz), Gamma (>32 Hz) [13], and their combinations. The entire EEG recordings are bandpass-filtered. Next the features are computed for the filtered signals, and then extracted for all 0.5 segments.

2.3. Designing the cascade

To reduce the computational load in the training phase, background waveforms are randomly sampled from the data of each subject. The number of sampled background waveforms is 5 times the number of ETs for each subject. For subjects with a small number of ETs, at least 2000 background waveforms are extracted.

In the first step, locations of all the annotated ETs along with the sampled backgrounds are collected. All the abovementioned features are computed for all EEG segments in the training set.

Next the threshold is selected for each feature. To this end, the empirical cumulative density function (CDF) of each feature is determined, both for the background waveforms and the ETs. The threshold on the feature value is selected such that 99% of the ETs are preserved. The percentage of rejected background waveforms is computed for each feature. The features are sorted according to the rejection rate. The feature with the highest rejection is selected for the first step in the cascade. The same procedure is performed for the following stages, i.e., all the features are computed on the remaining data from the first stage, and the top feature which leads to the highest background rejection rate is selected and applied at the second step, etc. Thresholding steps are added to the cascade accordingly, till the rejection rate stops increasing significantly or till the percentage of rejected spikes falls below a predefined value. Since 1% of ETs is lost after each stage, we choose 10 to be the maximum number of rejection steps, so that about 10% of the ETs are rejected.

2.4. Evaluating the performance of the cascade

After selecting the features and the corresponding thresholds for each step, the performance of the cascade is tested on the entire dataset. We extract waveforms by applying a sliding window with 75% overlap. After computing a feature value for each waveform, we apply the thresholds determined in the training stage. A waveform that is not rejected might correspond to an ET or background waveform. To distinguish both, additional classification would need to be applied, potentially by more complex and powerful classification methods. We compute the background rejection rate after each step. The performance for the entire cascade is evaluated by the final specificity and sensitivity.

3. RESULTS AND DISCUSSION

The CDF of the most discriminative feature, applied in the first step of the cascade, is depicted in Fig. 4, both for the ETs and background waveforms. The vertical line indicates the threshold θ. By rejecting waveforms whose feature values are below θ, only 1% of the ETs will be rejected. From Fig. 4 it can also be seen that 62.48% of the background waveforms have feature values below θ. In summary, by rejecting waveforms whose feature values are below the threshold θ, 62.48% of the background waveforms will be removed, while 99% of the ETs are retained.

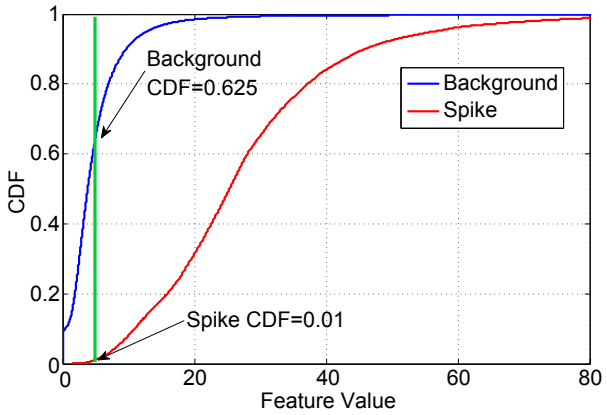

Fig. 4: Empirical CDF plot for the most discriminative feature (applied in the first step of the cascade), and the corresponding threshold θ.

The time needed to process all 19 channels of a 5 min EEG recording is listed in Table 1. We report the computational time for each category of features (applied separately, i.e., not in cascade) and for the 10-step cascade. In the initial steps of the cascade, the majority of the data is rejected. Therefore, the final steps of the cascade require less computational time. As a result, the overall time for the 10-step cascade is far less than the summation of the time needed for each feature separately. The computations were performed on a 2.7 GHz Intel Core i5 processor. The time is measured for the entire process, including loading the data, preprocessing and filtering, segmenting the data using a 75% overlapping sliding window, feature computation, applying the threshold, and saving the output.

In order to train the cascade, we determined the sequence of most discriminative features and selected appropriate thresholds for each of these features. Next we tested the resulting cascade of thresholding steps on the entire EEG dataset. The

Table 1: Processing time of each feature category, and the total processing time for the 10-step cascade, on a 5 min EEG data.

Feature	Processing time (min)
DWT	3.64
CWT	4.85
NLEO	3.7
All Voltage & Slope values	6.62
Line Length	3.23
10-step Cascade	9.87

training and test results are listed in Table 2. In all steps, the thresholds were selected such that 99% of the ETs were preserved. In the testing phase, the 10-step cascade is able to reject 98.65% of the background waveforms, while preserving 90.6% of the ETs.

The three most discriminative features happen to be extracted from the frequency band of 4–12 Hz, which includes the Theta and Alpha bands of EEG. Therefore, we can conclude that features in this frequency range yield better separation between ETs and background waveforms. Moreover, we observed that features computed in higher frequency bands yielded the lowest rejection rate. More precisely, in most cases the Gamma band resulted in the lowest rejection rate among other bands, for a particular feature.

The rejection rates after each step are shown in Fig. 5 both for the training and test data. As expected, the rejection rates increase after each step. However, the increase in rejection rate becomes smaller after each consecutive step, and gradually saturates.

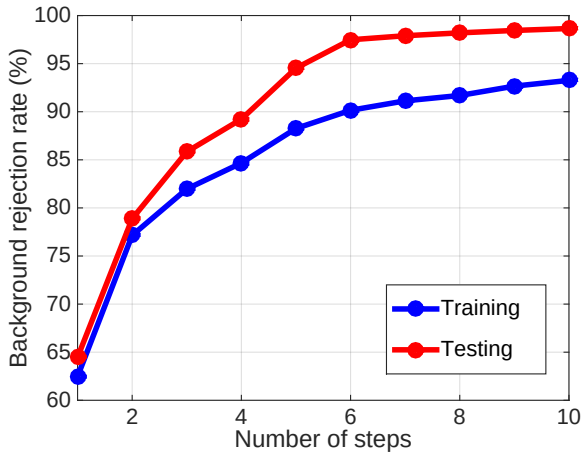

Fig. 5: The overall background rejection rate versus the number of steps taken.

We limited the steps of background rejection to 10, in order to retain most ETs (90.6%). From Fig. 5 it can be seen that by selecting the most salient feature at the first step, we can reject a high portion of background waveforms from the beginning of the cascade. In the training phase, we only analyze a small subset of the EEG of each patient, in order to limit the computational time. For testing purposes, we consider the entire EEG dataset of each patient. As there are many more background waveforms in the testing phase compared to the training phase, we expect a higher background rejection rate at testing comparing to training. As can be seen from Fig. 5 and Table 2, the rejection rate on the test dataset is indeed higher than on the training dataset.

Table 2: Selected features for each step of the cascade, and the overall background rejection rate after each step.

Step	Feature	Rejection (%) (Training)	Rejection (%) (Testing)
1	CWT (s=4, 4–12Hz)	62.48	64.47
2	Peak Voltage (4–12Hz)	77.15	78.88
3	DWT (D1, 4–12Hz)	81.97	85.84
4	NLEO (k=1, <4 Hz)	84.67	89.23
5	Rising Voltage (8–12Hz)	88.26	94.53
6	CWT (s=7, 0.1-64Hz)	90.15	97.48
7	NLEO (k=8, 0.1–64Hz)	91.13	97.9
8	DWT (A1, 0.1–64Hz)	91.69	98.2
9	CWT (s=12, 8–12Hz)	92.66	98.45
10	Rising Slope (4–8Hz)	93.26	98.65

4. CONCLUSIONS

In this paper, we proposed a method to perform fast multi-step background rejection on (interictal) EEG of epilepsy patients. Several features including morphological, energy, and wavelet measures were applied. By applying thresholds on these features consecutively, we formed a cascade of thresholding steps. Using a sufficiently large dataset consisting of several different subjects ensures that the cascade can generalize quite well for new EEG recordings of different signal to noise ratio.

We plan to extend the feature space in future work. Applying more diverse features will help in increasing the rejection rate at each step, by exploiting different characteristics of the EEG. One way to increase the feature space is to consider different types of mother wavelets, rather than using one single wavelet. Moreover, we plan to increase the threshold, such that fewer ETs would be lost in each stage. By setting higher thresholds and leveraging on more diverse EEG features, we hope to increase the length of cascade, and achieve higher sensitivity and specificity. In addition, applying the method on an even larger number of subjects, will provide more reliable performance characteristics of this method.

With the ultimate aim of developing an efficient ET detector, we plan to further process the waveforms that remain after background rejection, by means of more sophisticated machine learning algorithms. Such algorithms are typically vastly more computationally demanding. However, by filtering out most background waveforms by the thresholding cascade proposed in this paper, the overall computational complexity of the ET detection system will remain within reasonable limits.

5. REFERENCES

[1] G.E. Chatrian, L. Bergamini, M. Dondey, D.W. Klass, M. Lennox-Buchthal, and I. Petersen, "A glossary of terms most commonly used by clinical electroencephalographers," *Electroencephalogr Clin Neurophysiol*, vol. 37, no. 5, pp. 538–548, 1974.

[2] Jonathan J. Halford, "Computerized epileptiform transient detection in the scalp electroencephalogram: Obstacles to progress and the example of computerized {ECG} interpretation," *Clinical Neurophysiology*, vol. 120, no. 11, pp. 1909 – 1915, 2009.

[3] Antoine Nonclercq, Martine Foulon, Denis Verheulpen, Cathy De Cock, Marga Buzatu, Pierre Mathys, and Patrick Van Bogaert, "Cluster-based spike detection algorithm adapts to interpatient and intrapatient variation in spike morphology," *Journal of Neuroscience Methods*, vol. 210, no. 2, pp. 259 – 265, 2012.

[4] Shaun S. Lodder, Jessica Askamp, and Michel J.A.M. van Putten, "Inter-ictal spike detection using a database of smart templates," *Clinical Neurophysiology*, vol. 124, no. 12, pp. 2328 – 2335, 2013.

[5] Yung-Chun Liu, Chou-Ching K. Lin, Jing-Jane Tsai, and Yung-Nien Sun, "Model-based spike detection of epileptic eeg data," *Sensors*, vol. 13, no. 9, pp. 12536–12547, 2013.

[6] Jian Zhang, Junzhong Zou, Min Wang, Lanlan Chen, Chunmei Wang, and Guisong Wang, "Automatic detection of interictal epileptiform discharges based on time-series sequence merging method," *Neurocomputing*, vol. 110, pp. 35 – 43, 2013.

[7] Jing Jin, Justin Dauwels, Sydney Cash, and M Brandon Westover, "Spikegui: Software for rapid interictal discharge annotation via template matching and online machine learning," in *Engineering in Medicine and Biology Society (EMBC), 2014 36th Annual International Conference of the IEEE*. IEEE, 2014, pp. 4435–4438.

[8] Rosana Esteller, Javier Echauz, T. Tcheng, Brian Litt, and Benjamin Pless, "Line length: an efficient feature for seizure onset detection," in *Engineering in Medicine and Biology Society, 2001. Proceedings of the 23rd Annual International Conference of the IEEE*. IEEE, 2001, vol. 2, pp. 1707–1710.

[9] Sudipta Mukhopadhyay and G.C. Ray, "A new interpretation of nonlinear energy operator and its efficacy in spike detection," *Biomedical Engineering, IEEE Transactions on*, vol. 45, no. 2, pp. 180–187, 1998.

[10] J.H. Choi and T. Kim, "Neural action potential detector using multi-resolution teo," *Electronics Letters*, vol. 38, no. 12, pp. 541–543, 2002.

[11] Stéphane Mallat, *A wavelet tour of signal processing*, Academic press, 1999.

[12] Inan Güler and Elif Derya Übeyli, "Adaptive neuro-fuzzy inference system for classification of eeg signals using wavelet coefficients," *Journal of neuroscience methods*, vol. 148, no. 2, pp. 113–121, 2005.

[13] Marc R Nuwer, Dietrich Lehmann, Fernando Lopes da Silva, Shigeaki Matsuoka, William Sutherling, and Jean-François Vibert, "Ifcn guidelines for topographic and frequency analysis of eegs and eps. report of an ifcn committee," *Electroencephalography and clinical Neurophysiology*, vol. 91, no. 1, pp. 1–5, 1994.